

---

This is the **accepted version** of the journal article:

Pi i Boleda, Bernat; Bouzas, Mireia; Gaztelumendi, Nerea; [et al.]. «Chiral pH-sensitive cyclobutane beta-amino acid-based cationic amphiphiles : Possible candidates for use in gene therapy». *Journal of Molecular Liquids*, Vol. 297 (January 2020), art. 111856. DOI 10.1016/j.molliq.2019.111856

---

This version is available at <https://ddd.uab.cat/record/274089>

under the terms of the  license

1 **Chiral pH-Sensitive Cyclobutane  $\beta$ -Amino Acid-Based**

2 **Cationic Amphiphiles:**

3 **Possible Candidates for Use in Gene Therapy**

4  
5 **Bernat Pi-Boleda,<sup>1§</sup> Mireia Bouzas,<sup>1§</sup> Nerea Gaztelumendi,<sup>2</sup> Ona Illa,<sup>1</sup>**

6 **Carme Nogués,<sup>2</sup> Vicenç Branchadell,<sup>1</sup> Ramon Pons,<sup>\*3</sup> Rosa M.**

7 **Ortuño<sup>\*1</sup>**

8  
9 1: Departament de Química, Universitat Autònoma de Barcelona, 08193 Cerdanyola del

10 Vallès, Barcelona, Spain.

11 2: Departament de Biologia Cel·lular, de Fisiologia i d'Immunologia, Universitat

12 Autònoma de Barcelona, 08193 Cerdanyola del Vallès, Spain.

13 3: Departament de Tecnologia Química i de Tensioactius, Institut de Química Avançada

14 de Catalunya, IQAC-CSIC, c/ Jordi Girona, 18-26, 08034 Barcelona, Spain.

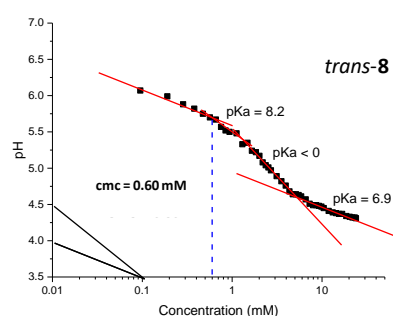
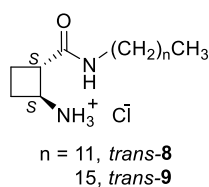
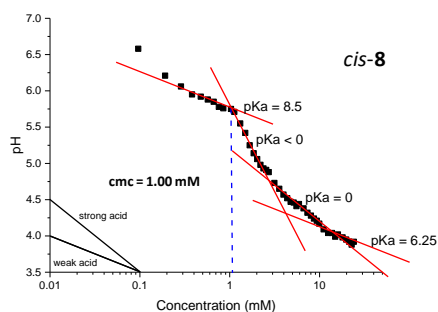
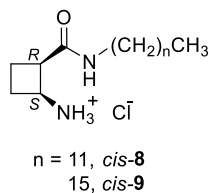
15

16

17

18 **ABSTRACT.**

19



20

21 Chiral *cis/trans* diastereomeric cationic amphiphiles have been synthesized and  
22 studied. They are based on  $\beta$ -amino acids and contain  $C_{12}$ - and  $C_{16}$ -alkyl chains,  
23 respectively, as hydrophobic tails while the polar head consists of an ammonium cation  
24 linked to a cyclobutane ring. Their physicochemical properties, such as the cmc (critical  
25 micellar concentration), the  $pK_a$ , the ratio of cationic versus non-ionic species, and the  
26 surface tension are strongly dependent on the pH of the medium. At the same time the  
27 aggregation state influences on the apparent  $pK_a$  values of the aggregates, with release  
28 of protons at the cmc whose values, as well as those of the adsorption effectiveness,  
29 account for their efficient surfactant behavior. A tail-length effect is manifest because  
30 surfactant cmc of compounds with a  $C_{16}$ -alkyl chain are smaller than the  $C_{12}$ -ones,  
31 although not as small as expected. On the other hand, while for  $C_{12}$ -surfactants the role  
32 of the stereochemistry on the physicochemical parameters is patent, it is not very clear  
33 for  $C_{16}$ -surfactants. The stereochemistry also determines the predominant mode of self-

34 assembly since the trend for *cis*-isomers is to form micelles or vesicles while *trans*-  
35 isomers preferably form fibers. CD spectroscopy confirmed the aggregation through the  
36 formation of intermolecular hydrogen bonds between the amide groups of the  
37 monomers. An alternative method to determine the cmc of these surfactants is provided  
38 by considering the relationship of the CD  $\lambda_{\max}$  with concentration, although it is  
39 restricted to those surfactants in which the chromophore is located in a chiral  
40 environment. Furthermore, the non- toxicity of the surfactants has been verified by the  
41 MTT assay. This characteristic, jointly with the efficiency and the good properties  
42 shown, the fact that the cationic species are present in a high concentration at  
43 physiological pH, as well as the weak acid behavior of the aggregates, confirm these  
44 amphiphiles as promising candidates to be used as non-viral vectors for gene therapy  
45 applications.

46

47

## 48        **1. INTRODUCTION**

49        Gene therapy has gained significant attention over the past two decades as a potential  
50        method for treating genetic disorders [1-5] as well as an alternative way to traditional  
51        chemotherapy used in treating cancer [6]. It mostly involves the use of DNA fragments  
52        that encodes a therapeutic protein or gene in order to replace a mutated gene. In these  
53        cases, DNA is packed within a vector forming DNA-vector complexes in order to  
54        protect the information of the chain and to get inside specific cells within the body [7].  
55        Depending on the temperature, the pH, or the ionic strength, a single DNA chain in  
56        solution could adopt different structures.

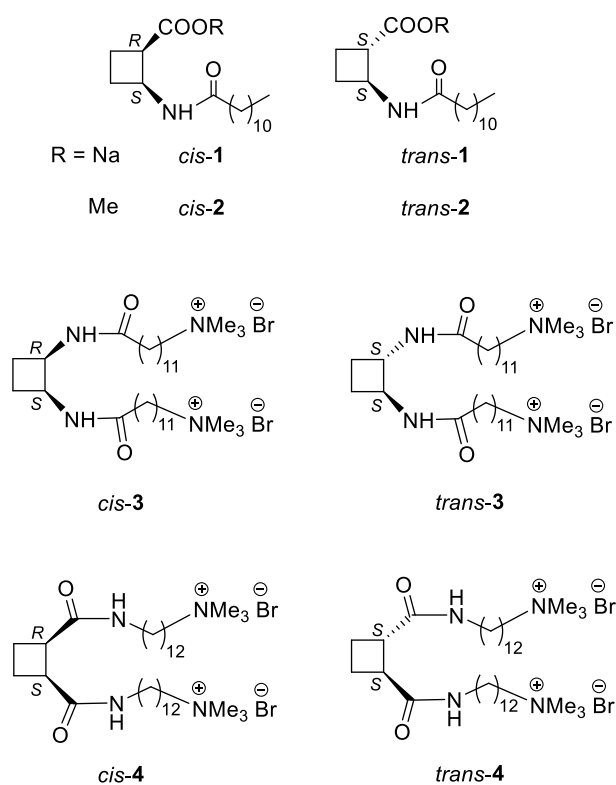
57        The role of chemists in the field of gene therapy is to design and prepare new non-  
58        viral vectors thus avoiding the risks derived of the work with virus materials. Special  
59        attention has been paid to cationic surfactants due to their properties [8]. Cationic polar  
60        heads can interact with negatively charged phosphate groups of the DNA while  
61        hydrophobic chains can stabilize the aggregates. In order to transfect into cells it is  
62        important to control DNA compaction and the neutralization of negative charges to  
63        avoid repulsive interactions with phospholipids in the cell membrane. One of the most  
64        studied surfactants is commercial CTAB (hexadecyl trimethylammonium bromide) [9-  
65        10]. It shows high efficiency compacting DNA compared with other shorter surfactants,  
66        but most trimethylammonium derivatives show cytotoxicity [11].

67        Amino acid-based surfactants are getting importance due to their good levels of  
68        biodegradability and biocompatibility [12-16]. The combination of amino acids or  
69        peptides with hydrocarbon chains of variable length has given rise to a variety of  
70        compounds with an amphiphilic structure and with good surfactant properties. Although  
71        most examples use natural  $\alpha$ -amino acids, the design of pH-sensitive amphiphiles can  
72        be achieved from synthetic amino acids. The possibility to tune the properties of the

73 surfactants depending on the pH of the medium confers on these compounds a great  
74 potential for biomedical applications [16-17]. Otherwise, the presence of amide groups  
75 can help the self-assembly of surfactants through intermolecular hydrogen bonding [18].

76 In our laboratories [19], different cyclobutane-containing anionic, **1** [20], or non-  
77 ionic, **2** [21],  $\beta$ -amino acid-based amphiphiles were synthesized and studied. Results  
78 pointed out the relevance of the relative stereochemistry and of the stereochemical  
79 constraints imposed by the cyclobutane ring on the aggregation properties of these  
80 compounds (Figure 1).

81



82

83 **Figure 1.** Anionic (**1**), non-ionic (**2**), and cationic (**3** and **4**) amphiphiles previously investigated  
84 in our laboratories.

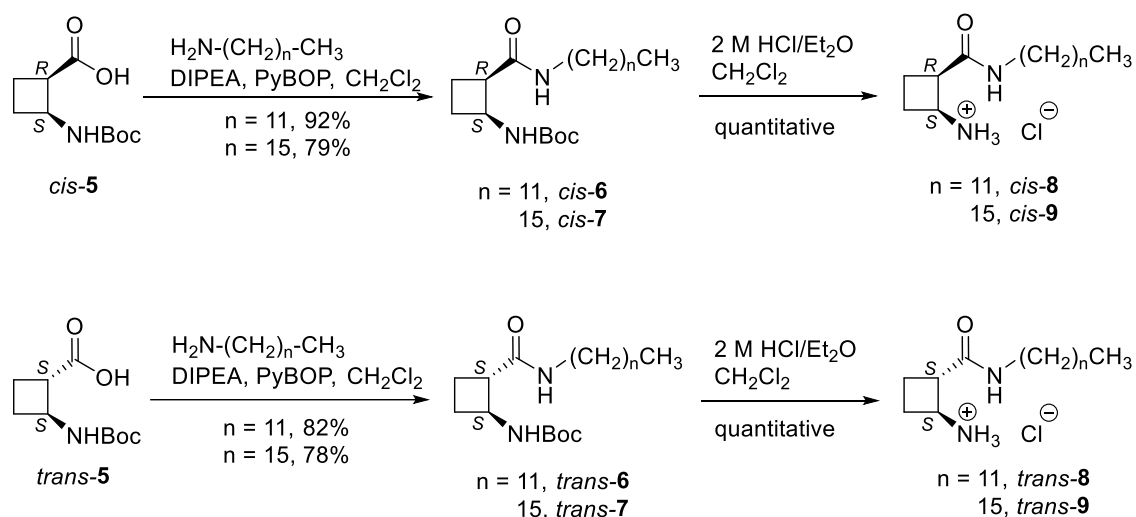
85

86 Cationic bolaamphiphiles based on chiral cyclobutane scaffolds, **3** and **4**, were also  
87 prepared and investigated concluding that regiochemistry (*N*- versus *C*-centered

88 derivatives) plays a minor role on the cmc value but determines the morphology of the  
89 supramolecular aggregates formed [22] (Figure 1).

90 In this paper, we describe the synthesis of four new cationic  $\beta$ -amino acid-based  
91 surfactants *cis*- and *trans*-**8**, and *cis*- and *trans*-**9** (Scheme 1). All these compounds are  
92 chiral and include two pairs of *cis/trans* diastereomers; in turn, **8** and **9** differ in the  
93 alkyl-chain length ( $C_{12}$  and  $C_{16}$ , respectively). Both the influence of the relative  
94 stereochemistry and of the chain length have been considered in their physicochemical  
95 characterization and in the analysis of the chiral supramolecular systems formed as  
96 surfactants. Special attention has been paid to the influence of the pH on these  
97 properties. Furthermore, bearing in mind the possibility of the future use of these  
98 surfactants as non viral vectors for gene therapy, preliminary studies on their  
99 cytotoxicity have been carried out. We present and discuss herein all the results  
100 obtained.

101



102

103 **Scheme 1.** Synthesis of the cationic amphiphiles *cis*- and *trans*-**8**, and *cis*- and *trans*-**9**.

104

105

106

## 107 2. EXPERIMENTAL SECTION

### 108 2.1 Synthesis of the amphiphiles.

109 The detailed synthesis and characterization of surfactants *cis*- and *trans*-**8**, and *cis*- and *trans*-**9**  
110 and their precursors (Scheme 1) are reported in the Supporting Information.

111

### 112 2.2 $pK_a$ Measurements.

113 The  $pK_a$  values were determined from the potentiometric titration of 1 mL of 5 mM aqueous  
114 surfactant solutions by using 5 mM NaOH aqueous solutions. The pH electrode was an ORION  
115 8103SC semimicro and the potentiometer was a Thermo Orion model 720A+. All titrations  
116 were conducted at  $25 \pm 0.1$  °C and under nitrogen atmosphere.  $pK_a$  was determined as the pH of  
117 the corresponding semi equivalence point. Once the titration is finished, a new titration with 5  
118 mM HCl is done to determine the reversibility. De-ionized water (milli-Q) was used to prepare  
119 the solutions.

120 The pH values of different concentrations of surfactant water solutions under nitrogen were  
121 measured using a pH electrode (model ORION 8103SC Ross Semimicro). Measurements were  
122 made at increasing concentrations of surfactant to minimize errors from possible contamination  
123 from the electrode. The acid–base equilibrium was modelled by Equation 1 for a weak base,  
124 assuming dilute ideal behavior and complete salt dissociation. This equation was obtained  
125 taking into account the equilibrium constant definition, mass and charge balances, and the ionic  
126 product of water.

127

128

$$129 \quad C_a = \left(1 + \frac{[H^+]}{K_a}\right) \left([H^+] - \frac{K_w}{[H^+]}\right) \quad (1)$$

130

131

132 The  $pK_a$  values both below the cmc (monomeric surfactant) and above the cmc (apparent  
133  $pK_a$ ) were evaluated by using this equation.

134

### 135 2.3 Surface Tension Measurements.

136 The surface tension was measured using a home-made pendant drop tensiometer as in reference  
137 22. Surface tension in acidic (0.01 M HCl) and basic conditions (0.01 M NaOH) have been  
138 compared with unbuffered aqueous solutions. When using Gibbs isotherm the values of  $n$  to  
139 estimating the area per molecule at cmc are 1 for both buffered conditions and undefined for the  
140 unbuffered conditions. We are aware of the problems with estimating area per molecule from



141 surface tension, however, we think that these values have a strong comparative meaning when  
142 compared to other in the literature, please refer to reference 22 and literature cited herein.

#### 143 *2.4 Cryogenic Transmission Electron Microscopy (cryo-TEM).*

144 A drop of the surfactant solution with 2.5 mM concentration was placed on a carbon-coated  
145 copper grid. Then, the sample-grid assembly was rapidly frozen using liquid ethane and kept at -  
146 180 °C during the imaging using liquid nitrogen. The images were acquired with Hitachi H-  
147 7000 microscope operating at 200 kV.

148

#### 149 *2.5 Computational Calculations.*

150 The structure of the surfactants in solution was optimized with DFT in water solution using  
151 M06-2X density functional [23] and 6-31G(d) level of theory. These calculations have been  
152 carried out using the Gaussian-09 program [24]. Circular dichroism spectra were calculated by  
153 taking the optimized structure of the monomer in water solution and calculating 30 excited  
154 states with Gaussian-09 using the TDDFT method [25-27] at the M06-2X/6-311++G(2df,2pd)  
155 level of theory.

156

#### 157 *2.6 Circular Dichroism (CD) Spectroscopy.*

158 0.5-5.0 mM samples of surfactants were prepared in water and measured in a 1 cm width quartz  
159 cuvette. CD spectra were recorded with JASCO-715 spectropolarimeter and were processed  
160 using Spectra Manager Software.

161

#### 162 *2.7 Ultraviolet – visible (UV - vis) Spectroscopy.*

163 The absorption was measured in a Hewlett Packard 8453 spectrophotometer in aqueous  
164 solutions in a range between 180 and 500 nm.

165

#### 166 *2.8 Biological Experiments.*

167 The MTT (3-(4,5-dimethylthiazol-2-yl)-2,5-diphenyltetrazolium bromide) assay [28], was used  
168 to analyze the cell viability and, proportionally, the surfactant toxicity. MTT (yellow color) is  
169 reduced by the mitochondrial enzymes to formazan, an insoluble purple crystal which  
170 absorbance can be read with a spectrophotometer after its solubilization by an organic solvent.  
171 The higher the absorbance value, the higher the enzymatic activity, and therefore the more  
172 number of living cells are present. In separate experiments, *HeLa* cells [29] were incubated in  
173 the presence of the different surfactants at about 50 µM concentration in water and MTT  
174 (Sigma-Aldrich) in a 0.1 mg/mL concentration was added. After 3 h of incubation at 37 °C in  
175 darkness, the MTT was removed and formazan crystals were dissolved using DMSO. The  
176 absorbance was recorded at 540 nm in an X3 Multilabel Plate Reader coupled to a PerkinElmer

177 2030 Manager control software. The experiments were replicated 4 times for each surfactant.  
178 The control experiment was performed under the same conditions but in the absence of a  
179 surfactant.

180 The normalization of the results was achieved considering the average of the absorbance  
181 value of the control population as 100% of cellular proliferation (Equation 2).

182

$$183 \quad \% \text{ Cell viability} = \frac{\text{Average Absorbance of treated cells}}{\text{Average Absorbance of non-treated cells}} \times 100 \quad (2)$$

184

### 185 **3. Results and Discussion**

186

#### 187 3.1 Synthesis of the amphiphiles.

188 *cis*- and *trans*-Diastereoisomers of compounds **8** and **9** were synthesized from the  
189 appropriate and partially protected amino acids *cis*- and *trans*-**5**, respectively, by means  
190 of analogous synthetic routes (Scheme 1). These amino acids were prepared, in turn, in  
191 an enantioselective manner as previously described [30-31].

192 Condensation of acid *cis*-**5** [30] with dodecylamine, in the presence of  
193 diisopropylamine (DIPEA) and (benzotriazol-1-yloxy)tripyrrolidinophosphonium  
194 hexafluorophosphate (PyBOP) as a coupling agent, afforded *cis*-**6** in 92% yield for the  
195 two steps. Similarly, condensation with hexadecylamine led to *cis*-**7** in 79% yield.  
196 Subsequently, quantitative deprotection of the respective amines by acidolysis of the  
197 Boc carbamate with 2 M HCl in Et<sub>2</sub>O provided cationic amphiphiles *cis*-**8** and *cis*-**9**,  
198 respectively. Following similar synthetic routes starting from *trans*-**5** [31], the  
199 diastereomers *trans*-**8** and *trans*-**9** were prepared in 82 and 78% yield, respectively.

200

201 3.2 Determination of the pK<sub>a</sub> of the surfactants and study of the pH dependence.

202 The  $pK_a$  of the surfactants investigated was determined by using two different and  
203 complementary techniques: (a) Measurement of the pH at various surfactant  
204 concentrations; (b) acid-base titration with sodium hydroxide and retro-titration with  
205 hydrochloric acid. Surfactants **8** and **9** present an acid-base equilibrium in aqueous  
206 medium that is the average of several equilibria involving ionic or non-ionic monomers  
207 and aggregates, which depend on the pH of the medium and the concentration of the  
208 surfactant.

209

210 3.2.1 Measurement of the pH at diverse surfactant concentrations.

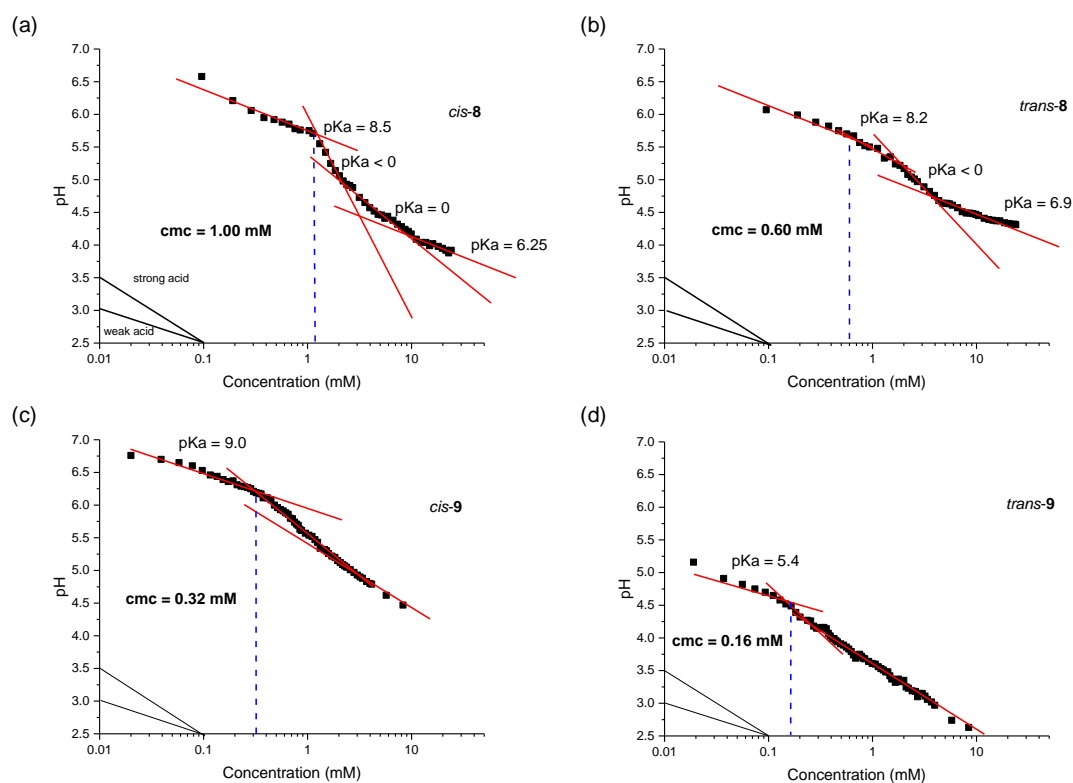
211 First, the dependence of the pH on the concentration of surfactant was investigated at 25  
212 °C. The obtained plots are shown in Figure 2 and from data therein, the relation of  $pK_a$   
213 with respect to the concentration of surfactant was determined according to Equation 1  
214 in the Experimental Section.

215 For pH-sensitive amphiphiles, at the extremes of concentration, the pH values  
216 follow the slope of 0.5 expected for weak acids, with  $pK_a$  corresponding to the  
217 monomers at low concentrations and to the average of monomers and micelles above  
218 the cmc (Figure 2). The onset of micellization is marked by the first change of slope,  
219 which corresponds to the critical micellar concentration (cmc). Indeed, when the  
220 formation of micelles occurs, a release of protons is produced due to the apparent  $pK_a$   
221 change of the micelle with respect to the monomer [17] The dependence of the  $pK_a$   
222 values on the concentration, for each surfactant, is detailed in the Supporting  
223 Information (figure S1) .

224 Comparing diastereomeric surfactants *cis*- and *trans*-**8**, both with a  $C_{12}$ -alkyl chain,  
225 the  $pK_a$  values before the cmc are very similar: 8.5 for *cis*-**8** and 8.2 for *trans*-**8** (Figure  
226 2). Therefore, it seems that *cis/trans* stereochemistry does not exert a significant

227 influence on the behavior of the monomeric surfactants. Nevertheless, the slightly  
 228 weaker acidity of the *cis* isomer could be understood by the possibility of hydrogen  
 229 bonding between a proton of the ammonium cation and the oxygen of the carbonyl  
 230 group in the amide (see Figure 6 below). This possibility does not exist in the *trans*  
 231 stereoisomer. These values show that both surfactants are weak acids and their structure,  
 232 cationic or non-ionic, will depend on the pH of the solution. However, these surfactants  
 233 are more acid than alkylammonium chlorides (DAC), of use in gene therapy, which  $pK_a$   
 234 has been determined at several concentrations dodecylamine  $pK_a=8.8$  at 5 mM, or  
 235  $pK_a=9.16$  at 2 mM, while tetradecylamine has a  $pK_a=7.56$  at 2 mM [32]. Taking into  
 236 account that the pH of the human blood is around 7.4, we can expect that, under  
 237 physiological conditions, *cis*- and *trans*-8 will be mostly in the protonated form.

238



239

240 **Figure 2.** Plots of pH versus surfactant concentration for: (a) *cis*-8, (b) *trans*-8, (c) *cis*-9, (d)

241

*trans*-9. Measurement at 25 °C.

242

243 The situation is different for *cis*- and *trans*-**9** bearing a C<sub>16</sub>-alkyl chain. Indeed, *cis*-**9**  
244 presents a pK<sub>a</sub> 9.0 before the cmc while *trans*-**9** shows a very low pK<sub>a</sub>, around 5.4. This  
245 unexpected behavior could suggest that, in this case, stereochemistry plays a very  
246 important role in the acidity of the proton, in contrast with surfactants *cis*- and *trans*-**8**  
247 with a shorter carbon chain. Surfactant *trans*-**9** was the less soluble and, indeed, some  
248 turbidity was observed at high concentration (5 – 10 mM) while making the  
249 measurements. This suggests the possible formation of oligomers involving both  
250 cationic and non-ionic species.

251 Otherwise, a pK<sub>a</sub> shift depending on the surfactant concentration was observed in all  
252 cases (Figure 2 and Figure S1 in the Supporting Information). After the cmc, the pK<sub>a</sub>  
253 value decreases, *cis*-**8** presenting a higher pK<sub>a</sub> shift than that shown for *trans*-**8**. Thus,  
254 these compounds can behave as two different weak acids, as monomeric molecules  
255 before the cmc and as micelles after the cmc. A similar behavior was observed for  
256 diastereomers *cis*- and *trans*-**9**, although their lower solubility made difficult the study  
257 at high concentration.

258 The pK<sub>a</sub> shift of molecules undergoing aggregation has been extensively studied [33-  
259 34], and two main contributions to this fact were identified. One contribution comes  
260 from the virtual charge effect due to a discontinuity in dielectric constant at the micelle  
261 surface [35] and a second contribution comes from the polar heads interaction where  
262 some protons are released to the solution in order to stabilize the aggregates.

263 Once molecules begin to self-assemble, the pH of the solution starts to decrease with  
264 a higher slope (Figure 2). From the intersection of the two lines, the cmc value is  
265 obtained: 1.0 mM and 0.60 mM for *cis*-**8** and *trans*-**8**, respectively. Smaller values were  
266 obtained for longer-chain surfactants **9** with cmc 0.32 mM and 0.16 mM for *cis*-**9** and  
267 *trans*-**9**, respectively. DAC, a cationic surfactant with similar chain length, presents a

268 cmc of 9 mM (pH 7) and 12 mM (pH 5) at 25 °C [36], which are higher values than  
269 those for **8** and **9**. Therefore, the presence of the cyclobutane unit and the amide bond  
270 seems to have a significant role on those values. This finding seems to contradict what  
271 was found in the case of anionic surfactants with polar heads also containing  
272 cyclobutane and amide bond but which cmc value did not change appreciably with  
273 respect to the a carboxylate of the same chain length (i.e. 12 mM for sodium laurate).

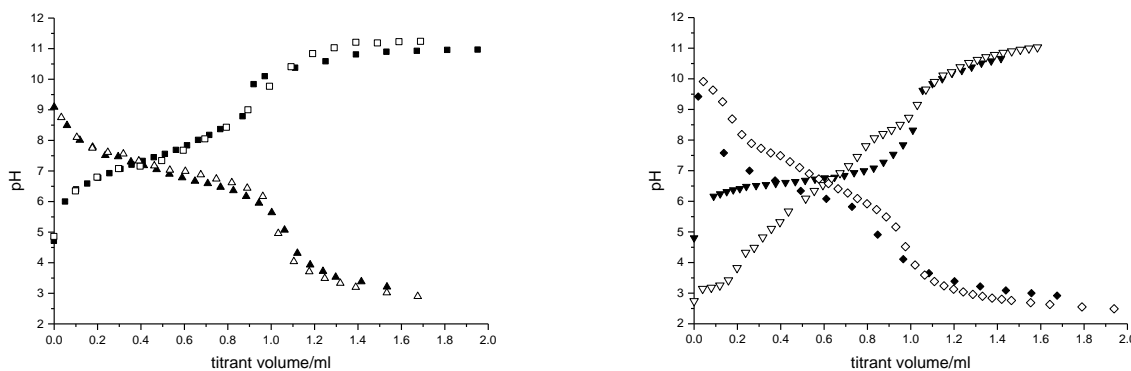
274 Moreover, the charge distribution in function of the concentration was determined  
275 for each surfactant by plotting  $[\text{NH}_3^+]/[\text{R-NH}_2]=[\text{H}^+]/K_a$  versus concentration (see  
276 Figure S2 in the Supporting Information). These graphics provide information about the  
277 behavior of these surfactants as acids. All of them have a maximum of charge at the  
278 cmc point. Before the cmc, each surfactant behaves as a normal weak acid but, once the  
279 cmc is reached, the amount of cationic species divided by the amount of non-ionic  
280 species ( $\text{R-NH}_3^+/\text{R-NH}_2$ ) starts to decrease in order to stabilize the aggregates and to  
281 reduce electrostatic repulsion between the molecules. It is interesting to note that, for  
282 *trans-9*, the charge ratio presents values between 3 and 5 showing that the concentration  
283 of the cationic surfactant is only 3-5 times higher than the concentration of the non-  
284 ionic surfactant. This ratio is much higher for the other surfactants studied.

285 The behavior of these amphiphiles could be interesting in medicinal chemistry,  
286 because changes in the protonation state would lead to changes the in headgroup area  
287 and, as a result, in their aggregation state. Surfactants with this type of properties were  
288 shown to be efficient vectors for gene therapy because the release of DNA into the cells  
289 is improved and, consequently, the level of gene transfection may be increased [37].

290

291 3.2.2. Acid-base titrations.

292 As a second methodology to determine the  $pK_a$ , acid-base titration of the surfactant  
293 aggregates with aqueous NaOH and subsequent retro-titration with HCl were carried  
294 out. The resultant curves for each surfactant are shown in Figure 3.  
295



296  
297 **Figure 3.** Titration curves of 5 mM aqueous solutions of *cis*-**8** (full squares), *trans*-**8** (open  
298 squares) and the corresponding back-titrations (full and open triangles respectively), *cis*-**9** ( full  
299 down triangles) and *trans*-**9** (open down triangles) and the corresponding back-titrations (full  
300 and open diamonds respectively), at 25 °C.

301

302 The  $pK_a$  values can be obtained from the pH at the half-equivalence point, and refer  
303 to the aggregate, which contains a 1:1 ratio of cationic and non-ionic species. At the end  
304 of the first titration with NaOH, the obtained aggregate consists mostly of non-ionic  
305 surfactants, while at the end of the retro-titration with HCl, the aggregate will be mainly  
306 made by cationic surfactants.

307 We can observe that the  $pK_a$  of these aggregates depends mainly on the length of the  
308 chain. The  $pK_a$  of the half-charged aggregates for the  $C_{12}$ -alkyl chain surfactants **8** is  
309  $7.2 \pm 0.2$  without significant influence of the stereochemistry while the  $pK_a$  for the  $C_{16}$  -  
310 surfactants is  $6.6 \pm 0.1$  for the *cis* stereoisomer and smaller ( $5.9$  in the direct titration and  
311  $7.1$  for the back-titration) for the *trans*- stereoisomer.

312 Looking at the profiles of the titration curves, we can conclude that for *cis-8*, *trans-8*  
313 and *cis-9* there is a clear equivalence point while for *trans-9* the equivalence point is  
314 less defined. Moreover, there is not a buffering effect with this molecule and the pH  
315 changes at almost constant slope (with some unexpected buffering effect at pH around  
316 3-3.5). This different behavior could be due to the presence of strongly different  
317 aggregates than in the other cases. That means that the starting aggregate is different  
318 from the others, as was observed in the previous  $pK_a$  measurements. Furthermore, once  
319 the non-ionic aggregate is obtained and the retro-titration is carried out, the profile of all  
320 the surfactants is quite similar, showing perfectly the two equivalence points. As  
321 observed in Figure 3, once the non-ionic aggregate has been formed, surfactant *trans-9*  
322 behaves as the others remarking the strong influence of the starting aggregate on the pH  
323 measurements. This difference seems a bit contradictory in the present case, since the  
324 passage through an insoluble phase would allow to reaching a thermodynamic state.

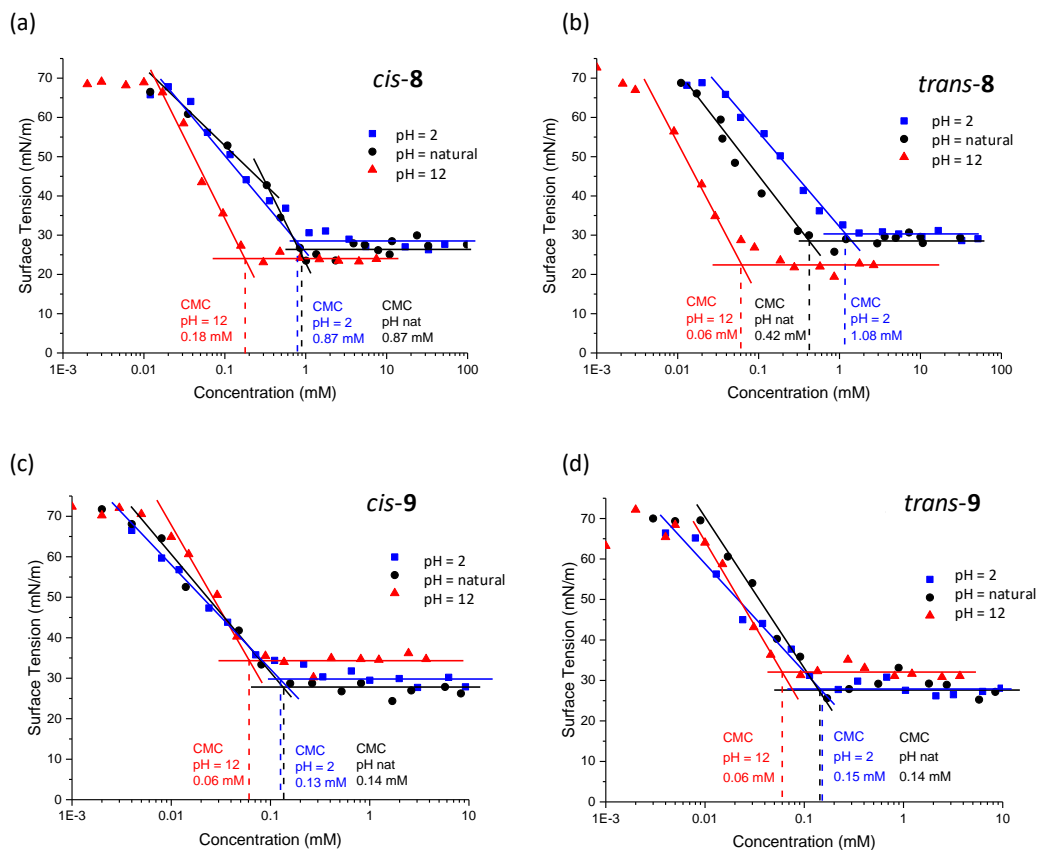
325

### 326 3.3 Surface tension measurements.

327 As stated before, these pH-sensitive surfactants are not purely cationic, but they are a  
328 mixture of cationic and non-ionic species depending on the pH. Therefore, in order to  
329 study their surfactant behavior, different measurements of the surface tension ( $\gamma$ ) were  
330 carried out at fixed pH values under buffered conditions or unbuffered (pH changing  
331 with surfactant concentration) conditions (see the Experimental Section). Plots of the  
332 surface tension versus surfactant concentration at three different pH values are shown in  
333 Figure 4. From these graphics, the parameters characterizing the surface properties of  
334 these surfactants, at 25 °C and different pH values, could be determined (Table 1).

335





336

337 **Figure 4.** Plot of surface tension versus surface concentration for *cis*-8 (a), *trans*-8 (b), *cis*-9  
 338 (c), and *trans*-9 (d) at pH 2 (blue), natural (black) and 12 (red).

339

340 The four compounds behave as good surfactants because they reduce the surface  
 341 tension from 70 to less than 40 mN/m, which has been taken as an indication of  
 342 saturation of the water-air interface with hydrocarbon tails [38]. In Figure 4, the cmc  
 343 values at each pH were determined, for each surfactant, as the intersection of the two  
 344 fitting straight lines in the plots of  $\gamma$  versus concentration. From the slope of the  
 345 curve just before the cmc, the Gibbs surface excess ( $\Gamma_{max}$ ) at the air-surface  
 346 corresponding to the cmc was obtained. From this value, the area per molecule ( $A_m$ )  
 347 at the surface could be calculated at pH=2 and pH=12. (See the Experimental  
 348 Section).

349

350

351  
352

**Table 1. Surface Properties of Surfactants *cis*- and *trans*-8, and *cis*- and *trans*-9 in Water at 25 °C.**

surfactant	pH	surface excess $\Gamma_{\max}$ ( $\mu\text{mol}/\text{m}^2$ )	area $A_m$ ( $\text{\AA}^2$ )	Effectiveness $\Pi_{\text{cmc}}$ (mN/m)	cmc (mM)
<i>cis</i> -8	2	4.1±0.2	41±4	41.5±1	0.87±0.15
	natural	6.7-3.4	---	46.8±2	<b>0.87±0.15</b>
	12	7.3±0.3	23±2	48.0±1	0.18±0.03
<i>trans</i> -8	2	4.2±0.2	40±4	40.8±1	1.08±0.10
	natural	4.6-2.3	---	44.3±2	<b>0.42±0.05</b>
	12	7.6±0.3	22±2	49.9±1.5	0.08±0.04
<i>cis</i> -9	2	4.3±0.2	39±4	44.6±1	0.13±0.02
	natural	5.0-2.5	---	44.6±2	<b>0.14±0.02</b>
	12	7.5±0.3	22±2	37.4±1	0.06±0.01
<i>trans</i> -9	2	4.2±0.2	39±4	43.6±1	0.14±0.02
	natural	6.2-3.1	---	44.4±2	<b>0.15±0.02</b>
	12	7.8±0.3	21±2	40.2±1	0.06±0.01

353  
354

355 At natural pH, for each surfactant, a mixture of species adsorbed at the surface is  
356 expected. Then, at this pH,  $A_m$  has not been determined, because of the lack of physical  
357 meaning. Looking at the obtained values at pH 2 and 12, we can observe that all the  
358 surfactants in the cationic state occupy around 40  $\text{\AA}^2$  while, when non-ionic, the area is  
359 around 22  $\text{\AA}^2$ , which corresponds to the minimum area that a tail alkyl chain occupies at  
360 the surface [39]. This result shows that in all cases they are able to saturate the surface  
361 of the solution with the corresponding carbon chains. This implies a high density of  
362 methyl terminal groups, which agree with the very low surface tension. In the case of  
363  $C_{16}$ -alkyl chain surfactant, the area per molecule of the neutral compounds is also low.  
364 However, it does not correspond to a so low surface tension and the reasons for this  
365 behavior are probably related to the previously observed anomaly for these  $C_{16}$ -  
366 compounds, that is, premicellar aggregation. The area per molecule of the cationic

367 surfactants is bigger than that of the non-ionic surfactants due to the repulsion between  
368 the charges. We can compare the values obtained here with the values obtained for  
369 trimethyl ammonium bromides and chlorides. For instance, the area per molecule  
370 determined for tetradecyl trimethyl ammonium bromide is 61 with a small reduction to  
371 59 in the presence of NaBr at 0.1 M. Chloride salts produce smaller area per molecule  
372 as deduced for dodecyl trimethyl ammonium chloride in 0.1M NaCl ( $38 \text{ \AA}^2$ ) or the  
373 longer chain hexadecyl trimethyl ammonium chloride in 0.1 M NaCl ( $46 \text{ \AA}^2$ ) [38].  
374 Surprisingly, the present surfactants show an area per molecule at full protonation  
375 comparable to the dodecyl trimethyl ammonium chloride with small or nil increment  
376 due to the bulky cyclobutane scaffold.

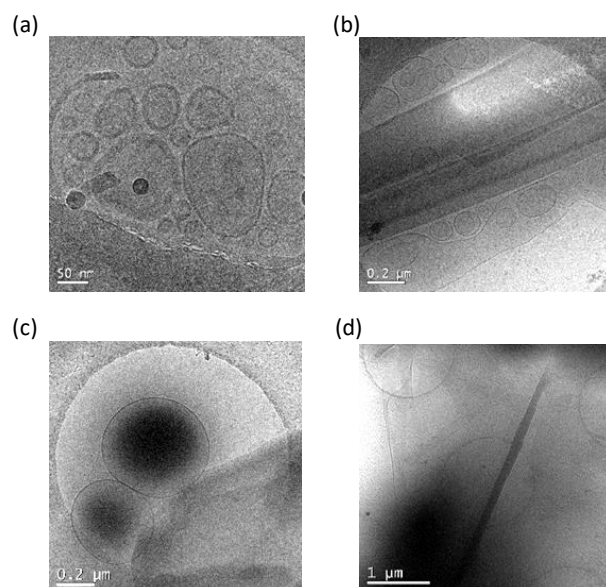
377 Special attention has to be paid to the obtained cmc values because they will mark  
378 the working concentrations for a possible further study of the interaction with DNA. At  
379 pH 2, both *cis* and *trans* diastereomers have a very similar cmc value: around 1 mM for  
380 *cis*- and *trans*-**8** and around 0.15 mM for *cis*- and *trans*-**9**. The behavior of these  
381 cationic surfactants can be compared with commercial dodecyltrimethylammonium  
382 bromide (DTAB), with cmc 16 mM at 25 °C [40], and CTAB, with cmc 0.98 mM, at 25  
383 °C [41]. For surfactants **8** and **9**, the difference in the cmc value while increasing the  
384 alkyl chain length from 12 to 16 carbon atoms is smaller than in the case of DTAB  
385 and CTAB. This is probably due to the presence of the cyclobutane moiety and points  
386 out that surfactants **8** and **9** are more efficient than the commercial ones. Therefore, at  
387 pH 2, having only cationic surfactants, stereochemistry seems not to play any  
388 significant role. Nevertheless, at pH 12, the cmc values of the compounds give the  
389 impression of being more dependent on the stereochemistry and on the chain length. For  
390 the non-ionic surfactants, the cmc is 0.18 mM for *cis*-**8**, while cmc is 0.06 mM for  
391 *trans*-**8**. Then, the *trans* isomer seems to be more efficient than the *cis* one. However,

392 for both *cis*- and *trans*-**9** the cmc is around 0.06 mM. So, in this case, the length of the  
393 chain has more influence on the solubility and, consequently, on the cmc value than the  
394 stereochemistry. Therefore, both diastereomers behave similarly as non-ionic  
395 surfactants at this pH. Finally, at natural pH, where there is a mixture of cationic and  
396 non-ionic surfactant, the cmc values appear to have the same behavior as at pH 2, as  
397 observed in Table 1, and can be compared with the obtained ones when measured in the  
398 bulk of the solution. It is noteworthy the different behavior of *trans*-**9** with respect to pH  
399 and surface tension. While in surfactants **8** former there are strong differences between  
400 both stereoisomers, for surfactants **9** there are not very significant differences.  
401 Anomalous trends in the dependence of cmc with chain length have been previously  
402 observed, particularly in the case of gemini surfactants [42]. In those cases, the decrease  
403 of cmc with chain length is smaller than for classical surfactants and, even increases of  
404 cmc have been observed for  $C_{16}$ -alkyl chain surfactants compared with  $C_{12}$ -ones. This  
405 anomalous behavior has been attributed to the formation of premicellar aggregates.  
406 Although the present structures are by no means gemini, it is not unconceivable that a  
407 dimer could behave in similar way as to a gemini surfactants.

#### 408 3.4 Cryo-TEM Studies.

409 The morphology of the aggregates formed by these four surfactants above the cmc, at  
410 three different pH values (2, natural and 12), was studied by using cryo-TEM at  $-180$   
411  $^{\circ}\text{C}$ . Selected cryo-TEM images are shown in Figure 5. (For a more complete set of cryo-  
412 TEM micrographs, see the Supporting Information, figures S3-S6). The images  
413 obtained showed irregular aggregates along with some vesicles and/or fibers with  
414 different size. Nevertheless, some trends were perceived allowing us to conclude that,  
415 independently of the pH, stereochemistry has some influence on the morphology of the  
416 aggregates and that *cis* surfactants seem to self-assemble preferably forming vesicles,

417 sometimes as multilayer aggregates, while *trans* surfactants, in addition to vesicles,  
418 form fibers at basic pH.  
419



420

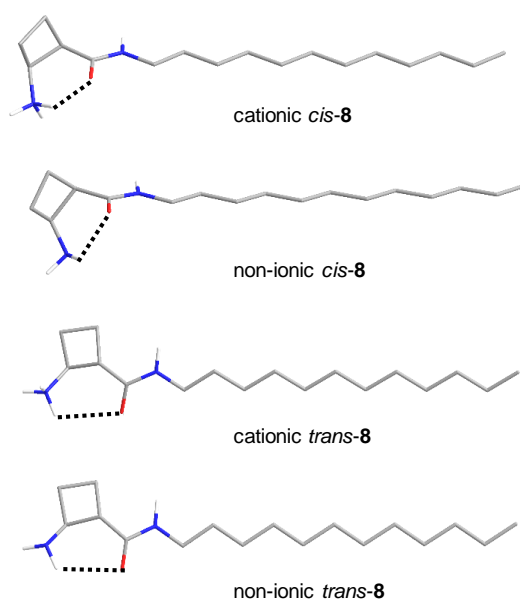
421 **Figure 5.** Selected cryo-TEM micrographs of a) *cis-8* at natural pH, b) *trans-8* at pH 12, c) *cis-9*  
422 at pH 2, d) *trans-9* at pH 12.

423

424 3.5 Computational calculations.

425 In order to gain insight in the structural features of monomeric surfactants and their  
426 ability to form intramolecular hydrogen bonds, computational calculations were carried  
427 out. The predicted structures are shown for *cis*- and *trans-8* in Figure 6. The same  
428 geometry of the polar head was found for *cis*- and *trans-9*, respectively. Distances of  
429 hydrogen bonds between the carbonyl oxygen of the amide and hydrogen from the free  
430 amine or the ammonium cation are listed in Table 3. Cationic *cis*-isomers form stronger  
431 intramolecular hydrogen bonds than non-ionic surfactants *cis-8* and *cis-9*. As expected,  
432 the *trans* diastereomers present very weak intramolecular hydrogen-bonding both in the  
433 cationic and non-ionic species. The length of the alkyl chain also plays a role in  
434 agreement with the lower solubility in water of surfactants **9** with respect to that of **8**.

435



436

437 **Figure 6.** Calculated structures of cationic and non-ionic species for surfactants *cis*- and *trans*-  
 438 **8**. Non-polar hydrogen atoms are omitted for clarity.

439

440

441 **Table 3. Hydrogen-bond Distances in Monomeric Surfactants *cis*- and *trans*-**8**,**  
 442 **and *cis*- and *trans*-**9**.**

Surfactant	C=O····H-N (cationic) (Å)	C=O····H-N (non-ionic) (Å)
<i>cis</i> - <b>8</b>	1.979	2.469
<i>trans</i> - <b>8</b>	2.853	2.863
<i>cis</i> - <b>9</b>	2.042	2.639
<i>trans</i> - <b>9</b>	2.858	2.869

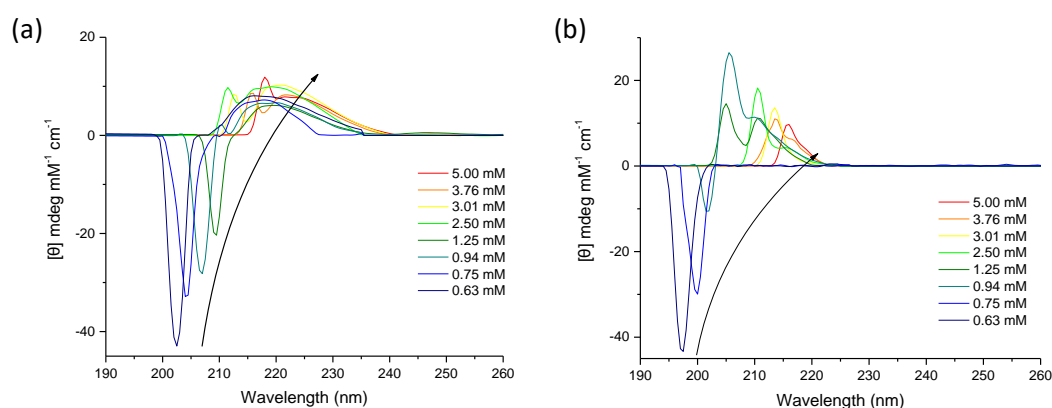
443

444

### 445 3.6. Circular Dichroism (CD) studies.

446 Aggregation of chiral surfactants into chiral aggregates can be followed using CD  
 447 spectroscopy [20,43-44]. Therefore, the analysis of the corresponding spectra between  
 448 200 and 250 nm would afford information about the chirality of the system [45] and one

449 could expect different CD spectra before and after the cmc. This assumption lies on the  
 450 fact that Cotton effects are extremely sensitive to changes in the chiral environment  
 451 close to the chromophore and to the interchromophoric interactions in supramolecular  
 452 aggregates [46]. The resultant CD spectra are shown in Figure 7. The shape and sign of  
 453 the CD signal was the same than that predicted by the theoretical CD spectrum of each  
 454 monomer of *cis*- and *trans*-**8** in solution (See the figure S7 in Supporting Information).  
 455

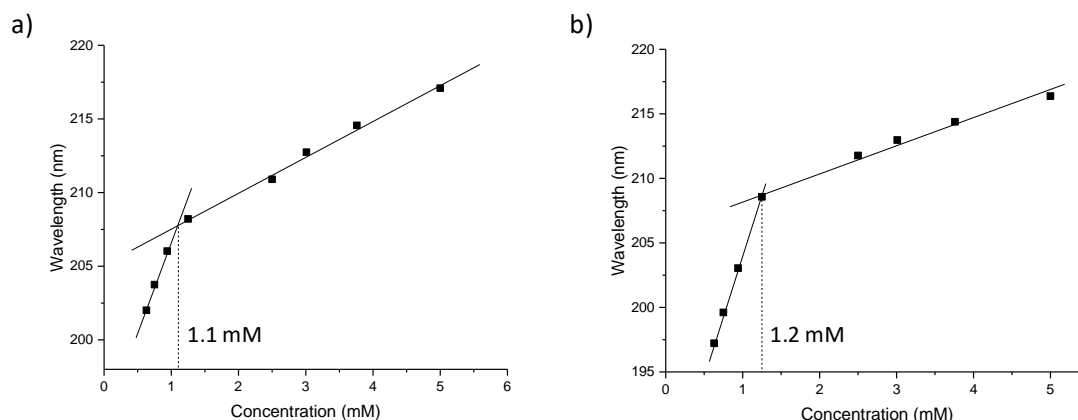


456  
 457 **Figure 7.** Experimental CD spectra at different concentrations of surfactants *cis*-**8** (a) and *trans*-  
 458 **8** (b).  
 459

460 When increasing the concentration of surfactant, the signal of the monomer is shifted  
 461 to longer wavelengths. The red shift could be attributed to the formation of aggregates  
 462 through the creation of hydrogen bonds involving the chromophore group, i.e. the  
 463 amide, that provokes a change in the transition energy [18,46].

464 Measurements of the UV-vis absorption of each surfactant in aqueous solution were  
 465 carried out (see figure S8 in the Supporting Information) and, in fact, a slight red shift  
 466 can be observed from low to higher concentrations, in agreement with CD results.  
 467 However,  $\lambda_{\max}$  in UV-vis is not the same as  $\lambda_{\max}$  in CD because there is a change from  
 468 single molecules to aggregates at the cmc, as can be appreciated in the representation  
 469 of CD  $\lambda_{\max}$  values in function of the surfactant concentration (Figure 8).

470



471

472 **Figure 8.** Plots of CD  $\lambda_{\max}$  versus concentration of surfactant *cis-8* (a) and *trans-8* (b).

473

474 Both graphics show a sharp change in the slope at values closely related to those  
475 determined for the cmc in solution (see previous sections in this manuscript). Therefore,  
476 in these cases, CD spectroscopy can be used for the determination of the cmc because it  
477 is known that this parameter contains a range of concentrations and its true value can  
478 vary up to one order of magnitude depending on the method used and on the measured  
479 physical property [17,20]. The determination of the cmc of a surfactant by the change in  
480 UV-vis absorption related to the formation of aggregates had been already reported [47-  
481 49]. However, these techniques are based only on the intensity of the absorption and not  
482 on the  $\lambda_{\max}$  value and a clear peak in the spectra should be observed in order to  
483 determine the maximum. Even so, this technique is restricted to surfactants that self-  
484 assemble through a chromophore located in a chiral environment.

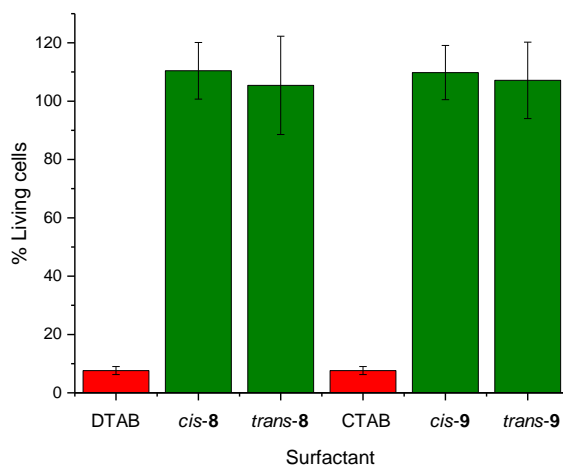
485 Surfactants *cis-* and *trans-9* were also investigated (see figure S9 in the Supporting  
486 Information). Nevertheless, due to their low solubility and, consequently, their low cmc  
487 value (around 0.1-0.2 mM) the method became limited to the study of a narrow range of  
488 concentrations and reliable conclusions could not be obtained.

489 3.7. Cytotoxicity of the surfactants.



490 Encouraged by the interesting properties found for surfactants **8** and **9** and focusing on  
491 the possibility to use them as non viral vectors for gene therapy, a preliminary  
492 investigation of their cytotoxicity was carried out by means of the MTT assay. Standard  
493 HeLa cells were used for this study. The 100% living cells was considered as the result  
494 of a control experiment performed in absence of the surfactants and under the same  
495 conditions as explained in the Experimental Section. The average toxicity results of four  
496 replicates for each surfactant are shown in Figure 9. We can observe that surfactants **8**  
497 and **9** are non-toxic in contrast to DTAB and CTAB, which are commonly used in  
498 biological experiments.

499



500

501 **Figure 9.** Toxicity results of the MTT assay with surfactants DTAB, *cis*- and *trans*-**8**, CTAB,  
502 *cis*- and *trans*-**9** using HeLa cells. Error bars represent standard deviations (SD) of four  
503 independent experiments.

504

#### 505 **4. Conclusions**

506 Two pairs of *cis/trans* diastereomeric  $\beta$ -amino acid-based cationic amphiphiles have  
507 been synthesized and studied. They contain  $C_{12}$ - and  $C_{16}$ -alkyl chains, respectively, as  
508 hydrophobic tails and the polar head consists of an ammonium cation linked to a

509 cyclobutane ring. The pH of the medium modulates their physicochemical properties,  
510 such as the cmc, the ratio of cationic versus non-ionic species and the surface tension  
511 magnitude. At the same time the aggregation state influences on the apparent  $pK_a$  values  
512 of the aggregates, with release of protons at the cmc. The cmc for all of them is lower  
513 than that for commercial DTAB and CTAB, which is probably due to the steric  
514 restrictions imposed by the cyclobutane unit. Moreover, the adsorption effectiveness is  
515 around 40 mN/m in all cases, which is in accordance with an efficient surfactant  
516 behavior. The tail-length influences the surfactant properties and those with a  $C_{16}$ -alkyl  
517 chain are better than those with a shorter tail. In terms of surface tension there is some  
518 effect of stereochemistry regarding the position of cmc for the  $C_{12}$ - derivatives, while  
519 there is no effect for  $C_{16}$ - or on the area per molecule. Aggregation influences on the  
520 apparent  $pK_a$  of these molecules with *trans*-**9** behaving as a much more acidic molecule  
521 than expected, but this particular behavior does not translate to other properties. The  
522 stereochemistry also determines the predominant mode of self-assembling since the  
523 trend for *cis*-isomers is to form micelles or vesicles while *trans*-isomers preferably form  
524 fibers. CD spectroscopy supports the formation of aggregates through intermolecular  
525 hydrogen-bonding between the amide groups of the monomers. Moreover, by  
526 considering the relationship of the CD  $\lambda_{max}$  with the concentration, an alternative  
527 method to determine the cmc of these surfactants is provided. This methodology could  
528 be general but is restricted to those surfactants in which the chromophore is located in a  
529 chiral environment. Finally, the non- toxicity of the surfactants has been verified by the  
530 MTT assay. This characteristic, jointly with the efficiency and the good properties  
531 shown, the fact that the cationic species are present in a high concentration at  
532 physiological pH, as well as the weak acid behavior of the aggregates, confirm these

533 amphiphiles as promising candidates to be used as non-viral vectors for gene therapy  
534 applications. Further investigation in this field is being carried out in our laboratories.

535

## 536 **ASSOCIATED CONTENT**

### 537 **Supporting Information**

538 Synthetic procedures, characterization, and  $^1\text{H}$  and  $^{13}\text{C}$  NMR spectra of the new  
539 compounds; charge distribution at different concentration of the surfactants; cryo-TEM  
540 micrographs of the surfactants at different pH values; calculated CD spectra for *cis*- and  
541 *trans*-**8**; CD and UV-vis absorption spectra of *cis*- and *trans*-**9**.

## 542 **AUTHOR INFORMATION**

### 543 **Corresponding Authors**

544 \*E-mail: [ramon.pons@iqac.csic.es](mailto:ramon.pons@iqac.csic.es) (R.P.).

545 \*E-mail: [rosa.ortuno@uab.es](mailto:rosa.ortuno@uab.es) (R.M.O.).

### 546 **ORCID**

547 Bernat Pi-Boleda: 0000-0003-1050-6788

548 Ona Illa : 0000-0001-7390-4893

549 Vicenç Branchadell : 0000-0003-3480-1669

550 Ramon Pons : 0000-0003-4273-9084

551 Rosa M. Ortuño: 0000-0001-7635-7354

### 552 **Present Address**

553 ☼ Kao Corporation, S.A.; Puig dels Tudons, 10, 08210 Barberà del Vallès, Barcelona,  
554 Spain

555 § Kern Pharma, S.L. ; Venus, 72, Pol. Ind. Colón II, 08228 Terrassa, Barcelona, Spain

556

557 **Notes**

558 The authors declare no competing financial interest.

559 **ACKNOWLEDGMENTS**

560 Financial support from MINECO (CTQ2016-77978-R, AEI/FEDER, UE, and  
561 CTQ2017-88948-P) is gratefully acknowledged. Ms. Imma Carrera is gratefully  
562 acknowledged for help with the surface tension measurements.

563

564 **REFERENCES**

- 
- [1] Cavazzana-Calvo, M. Gene Therapy of Human Severe Combined Immunodeficiency (SCID)-X1 Disease. *Science* **2000**, *288* (5466), 669–672.
- [2] Manno, C. S.; Pierce, G. F.; Arruda, V. R.; Glader, B.; Ragni, M.; Rasko, J. J.; Rasko, J.; Ozelo, M. C.; Hoots, K.; Blatt, P.; Konkle, B.; Dake, M.; Kaye, R.; Razavi, M.; Zajko, A.; Zehnder, J.; Rustagi, P. K.; Nakai, H.; Chew, A.; Leonard, D.; Wright, J. F.; Lessard, R. R.; Sommer, J. M.; Tigges, M.; Sabatino, D.; Luk, A.; Jiang, H.; Mingozzi, F.; Couto, L.; Ertl, H.C.; High, K. A.; Kay, M. A. Successful Transduction of Liver in Hemophilia by AAV-Factor IX and Limitations Imposed by the Host Immune Response. *Nat. Med.* **2006**, *12*, 342–347.
- [3] *Gene and Stem Cell Therapy*; Boyd, A. C., Ed.; Karger: Basel, New York, 2006.
- [4] Maguire, A. M.; Simonelli, F.; Pierce, E. A.; Pugh, E. N.; Mingozzi, F.; Bennicelli, J.; Banfi, S.; Marshall, K. A.; Testa, F.; Surace, E. M.; et al. Safety and Efficacy of Gene Transfer for Leber’s Congenital Amaurosis. *N. Engl. J. Med.* **2008**, *358*, 2240–2248.
- [5] Kaplitt, M. G.; Feigin, A.; Tang, C.; Fitzsimons, H. L.; Mattis, P.; Lawlor, P. A.; Bland, R. J.; Young, D.; Strybing, K.; Eidelberg, D.; et al. Safety and Tolerability of Gene Therapy with an Adeno-Associated Virus (AAV) Borne GAD Gene for Parkinson’s Disease: An Open Label, Phase I Trial. *Lancet* **2007**, *369*, 2097–2105.
- [6] Yang, Z. R.; Wang, H. F.; Zhao, J.; Peng, Y. Y.; Wang, J.; Guinn, B.-A.; Huang, L. Q. Recent Developments in the Use of Adenoviruses and Immunotoxins in Cancer Gene Therapy. *Cancer Gene Ther.* **2007**, *14*, 599–615.
- [7] *Advances in Genetics, Volume 89*; Friedmann, T., Dunlap, J. C., Goodwin, S. F., Eds.; Elsevier Inc.: Oxford, 2015.
- [8] *DNA Interaction with Polymers and Surfactants*; Dias, R. S., Lindman, B., Eds.; John Wiley & Sons, Inc: New Jersey, 2008.

- 
- [9] Carlstedt, J.; Lundberg, D.; Dias, R. S.; Lindman, B. Condensation and Decondensation of DNA by Cationic Surfactant, Spermine, or Cationic Surfactant-Cyclodextrin Mixtures: Macroscopic Phase Behavior, Aggregate Properties, and Dissolution Mechanisms. *Langmuir* **2012**, *28*, 7976–7989.
- [10] Grueso, E.; Cerrillos, C.; Hidalgo, J.; Lopez-Cornejo, P. Compaction and Decompaction of DNA Induced by the Cationic Surfactant CTAB. *Langmuir* **2012**, *28*, 10968–10979.
- [11] Pinnaduwege, P.; Schmitt, L.; Huang, L. Use of a Quaternary Ammonium Detergent in Liposome Mediated DNA Transfection of Mouse L-Cells. *Biochim. Biophys. Acta* **1989**, *985*, 33–37.
- [12] Pérez, N.; Pérez, L.; Infante, M. R.; García, M. T. Biological Properties of Arginine-Based Glycerolipidic Cationic Surfactants. *Green Chem.* **2005**, *7*, 540–546.
- [13] Infante, M. R.; Pérez, L.; Morán, M. C.; Pons, R.; Mitjans, M.; Vinardell, M. P.; Garcia, M. T.; Pinazo, A. Biocompatible Surfactants from Renewable Hydrophiles. *Eur. J. Lipid Sci. Technol.* **2010**, *112*, 110–121.
- [14] Pinazo, A.; Pons, R.; Pérez, L.; Infante, M. R. Amino Acids as Raw Material for Biocompatible Surfactants. *Ind. Eng. Chem. Res.* **2011**, *50*, 4805–4817.
- [15] Chandra, N.; Tyagi, V. K. Synthesis, Properties, and Applications of Amino Acids Based Surfactants: A Review. *J. Dispers. Sci. Technol.* **2013**, *34*, 800–808.
- [16] Foley, P.; Kermanshahi pour, A.; Beach, E. S.; Zimmerman, J. B. Derivation and Synthesis of Renewable Surfactants. *Chem. Soc. Rev.* **2012**, *41*, 1499–1518.
- [17] Mezei, A.; Pérez, L.; Pinazo, A.; Comelles, F.; Infante, M. R.; Pons, R. Self Assembly of pH-Sensitive Cationic Lysine Based Surfactants. *Langmuir* **2012**, *28*, 16761–16771.
- [18] Bordes, R.; Tropsch, J.; Holmberg, K. Role of an Amide Bond for Self-Assembly of Surfactants. *Langmuir* **2010**, *26*, 3077–3083.
- [19] Sorrenti, A.; Illa, O.; Ortuño, R. M. Amphiphiles in Aqueous Solution: Well Beyond a Soap Bubble. *Chem. Soc. Rev.* **2013**, *42*, 8200–8219.
- [20] Sorrenti, A.; Illa, O.; Pons, R.; Ortuño, R. M. Chiral Cyclobutane  $\beta$ -Amino Acid-Based Amphiphiles: Influence of *cis/trans* Stereochemistry on Solution Self-Aggregation and Recognition. *Langmuir* **2015**, *31*, 9608–9618.
- [21] Sorrenti, A.; Illa, O.; Ortuño, R. M.; Pons, R. Chiral Cyclobutane  $\beta$ -Amino-Acid Based Amphiphiles: Influence of *cis/trans* Stereochemistry on Condensed Phase and Monolayer Structure. *Langmuir* **2016**, *32*, 6977–6984.
- [22] Pi-Boleda, B.; Sorrenti, A.; Sans, M.; Illa, O.; Pons, R.; Branchadell, V.; Ortuño, R. M. Cyclobutane Scaffold in Bolaamphiphiles: Effect of Diastereoisomerism and Regiochemistry on Their Surface Activity Aggregate Structure. *Langmuir*, **2018**, *34*, 11424–11432.

- 
- [23] Zhao, Y.; Truhlar, D. G. The M06 Suite of Density Functionals for Main Group Thermochemistry, Thermochemical Kinetics, Noncovalent Interactions, Excited States, and Transition Elements: Two New Functionals and Systematic Testing of Four M06-Class Functionals and 12 Other Functionals. *Theor. Chem. Acc.* **2007**, *120*, 215–241.
- [24] Gaussian 09, Revision E.01, Frisch, M. J.; Trucks, G. W.; Schlegel, H. B.; Scuseria, G. E.; Robb, M. A.; Cheeseman, J. R.; Scalmani, G.; Barone, V.; Mennucci, B.; Petersson, G. A. *et al.* Gaussian, Inc., Wallingford CT, 2009.
- [25] Bauernshmitt, R.; Ahlrichs, R. Treatment of Electronic Excitations within the Adiabatic Approximation of Time Dependent Density Functional Theory. *Chem. Phys. Lett.* **1996**, *256*, 454–464.
- [26] Autschbach, J.; Ziegler, T.; van Gisbergen, S. J. A.; Baerends, E. J. Chiroptical Properties from Time-Dependent Density Functional Theory. I. Circular Dichroism Spectra of Organic Molecules. *J. Chem. Phys.* **2002**, *116*, 6930.
- [27] Stratmann, R. E.; Scuseria, G. E.; Frisch, M. J. An Efficient Implementation of Time-Dependent Density-Functional Theory for the Calculation of Excitation Energies of Large Molecules. *J. Chem. Phys.* **1998**, *109*, 8218-8224.
- [28] Mosmann, T. Rapid Colorimetric Assay for Cellular Growth and Survival: Application to Proliferation and Cytotoxicity Assays *J. Immunol. Methods* **1983**, *65*, 55-63.
- [29] Rahbari, R.; Sheahan, T.; Modes, V.; Collier, P.; Macfarlane, C.; Badge, R.M. A Novel L1 Retrotransposon Marker for HeLa Cell Line Identification. *BioTechniques*. **2009**, *46*, 277-284.
- [30] Izquierdo, S.; Rúa, F.; Sbai, F.; Parella, T.; Álvarez-Larena, A.; Branchadell, V.; Ortuño, R. M. *J. Org. Chem.* **2005**, *70*, 7963-7971.
- [31] Fernandes, C.; Pereira, E.; Faure, S.; Aitken, D. J. *J. Org. Chem.* **2009**, *74*, 3217-3220.
- [32] Matulis, D.; Bloomfield, V.A. Thermodynamics of the hydrophobic effect. I. Coupling of aggregation and pK<sub>a</sub> shifts in solutions of aliphatic amines. *Biophysical Chemistry* **2001**, *93*, 37-51.
- [33] Goldsipe, A.; Blankschtein, D. Molecular-Thermodynamic Theory of Micellization of pH-Sensitive Surfactants. *Langmuir* **2006**, *22*, 3547–3559.
- [34] Goldsipe, A.; Blankschtein, D. Titration of Mixed Micelles Containing a pH-Sensitive Surfactant and Conventional (pH-Insensitive) Surfactants: A Regular Solution Theory Modeling Approach. *Langmuir* **2006**, *22*, 9894–9904.
- [35] Söderman, O.; Jönsson, B.; Olofsson, G. Titration of Fatty Acids Solubilized in Cationic and Anionic Micelles. Calorimetry and Thermodynamic Modeling. *J. Phys. Chem. B* **2006**, *110*, 3288–3293.
- [36] Dai, Q.; Laskowski, J.S. The Krafft point of dodecylammonium chloride: pH effect. *Langmuir* **1991**, *7*, 1361-1364

- 
- [37] Fielden, M. L.; Perrin, C.; Kremer, A.; Bergsma, M.; Stuart, M. C.; Camilleri, P.; Engberts, J. B. F. N. Sugar-Based Tertiary Amino Gemini Surfactants with a Vesicle-to-Micelle Transition in the Endosomal pH Range Mediate Efficient Transfection in Vitro. *Eur. J. Biochem.* **2001**, *268*, 1269–1279.
- [38] Rosen, M. J.; Kunjappu, J. T. *Surfactants and Interfacial Phenomena*, 4th ed.; John Wiley & Sons, Inc.: New York, 2012.
- [39] Nagarajan, R. Self Assembly of Bola Amphiphiles. *Chem. Eng. Commun.* **1987**, *55*, 251–273.
- [40] Causi, S.; DeLisi, R.; Milioto, S.; Tirone, N. Dodecyltrimethylammonium Bromide in Water-Urea Mixtures. Volumes, Heat Capacities, and Conductivities. *J. Phys. Chem.*, 1991, *95*, 5664–5673.
- [41] Okuda, H.; Imae, T.; Ikeda, S. The Adsorption of Cetyltrimethylammonium Bromide on Aqueous Surfaces of Sodium Bromide Solutions. *Colloids and Surfaces* **1987**, *27*, 187–200.
- [42] Menger, F. M.; Littau, C. A. Gemini Surfactants: A New Class of Self-Assembling Molecules. *J. Am. Chem. Soc.* **1993**, *115*, 10083–10090.
- [43] Mohanty, A.; Dey, J. Effect of the Headgroup Structure on the Aggregation Behavior and Stability of Self-Assemblies of Sodium N-[4-(n-Dodecyloxy)benzoyl]-L-Aminoacidates in Water. *Langmuir* **2007**, *23*, 1033–1040.
- [44] El-Hachemi, Z.; Mancini, G.; Ribó, J. M.; Sorrenti, A. Role of the Hydrophobic Effect in the Transfer of Chirality from Molecules to Complex Systems: From Chiral Surfactants to Porphyrin/surfactant Aggregates. *J. Am. Chem. Soc.* **2008**, *130*, 15176–15184.
- [45] *Circular Dichroism: Principles and Applications*, 2nd ed.; Berova, N., Nakanishi, K., Woody, R. W., Eds.; Wiley-VCH: Weinheim, 1994.
- [46] Pescitelli, G.; Di Bari, L.; Berova, N. Application of Electronic Circular Dichroism in the Study of Supramolecular Systems. *Chem. Soc. Rev.* **2014**, *43*, 5211–5233.
- [47] Yu, D.; Huang, F.; Xu, H. Determination of Critical Concentrations by Synchronous Fluorescence Spectrometry. *Anal. Methods* **2012**, *4*, 47–49.
- [48] Tanhaei, B.; Saghatoleslami, N.; Chenar, M. P.; Ayati, A.; Hesampour, M.; Mänttari, M. Experimental Study of CMC Evaluation in Single and Mixed Surfactant Systems, Using the UV–Vis Spectroscopic Method. *Journal of Surfactants and Detergents*, 2013, *16*, 357–362.
- [49] Polavarapu, P. L.; Vijay, R. Chiroptical Spectroscopy of Surfactants. *J. Phys. Chem. A* **2012**, *116*, 5112–5118.